

Prediction of Obstructive Lung Disease from Chest Radiographs via Deep Learning Trained on Pulmonary Function Data

This article was published in the following Dove Press journal:
International Journal of Chronic Obstructive Pulmonary Disease

Joyce D Schroeder ¹
Ricardo Bigolin Lanfredi ²
Tao Li³
Jessica Chan¹
Clement Vachet ⁴
Robert Paine III⁵
Vivek Srikumar³
Tolga Tasdizen ²

¹Department of Radiology and Imaging Sciences, School of Medicine, University of Utah, Salt Lake City, UT, USA; ²Department of Electrical and Computer Engineering, Scientific Computing and Imaging Institute (SCI), University of Utah, Salt Lake City, UT, USA; ³School of Computing, University of Utah, Salt Lake City, UT, USA; ⁴Biomedical Imaging and Data Analytics Core, SCI, University of Utah, Salt Lake City, UT, USA; ⁵Division of Pulmonary and Critical Care Medicine, School of Medicine, University of Utah, Salt Lake City, UT, USA

Background: Chronic obstructive pulmonary disease (COPD), the third leading cause of death worldwide, is often underdiagnosed.

Purpose: To develop machine learning methods to predict COPD using chest radiographs and a convolutional neural network (CNN) trained with near-concurrent pulmonary function test (PFT) data. Comparison is made to natural language processing (NLP) of the associated radiologist text reports.

Materials and Methods: This IRB-approved single-institution retrospective study uses 6749 two-view chest radiograph exams (2012–2017, 4436 unique subjects, 54% female, 46% male), same-day associated radiologist text reports, and PFT exams acquired within 180 days. The Image Model (Resnet18 pre-trained with ImageNet CNN) is trained using frontal and lateral radiographs and PFTs with 10% of the subjects for validation and 19% for testing. The NLP Model is trained using radiologist text reports and PFTs. The primary metric of model comparison is the area under the receiver operating characteristic curve (AUC).

Results: The Image Model achieves an AUC of 0.814 for prediction of obstructive lung disease (FEV1/FVC < 0.7) from chest radiographs and performs better than the NLP Model (AUC 0.704, $p < 0.001$) from radiologist text reports where FEV1 = forced expiratory volume in 1 second and FVC = forced vital capacity. The Image Model performs better for prediction of severe or very severe COPD (FEV1 < 0.5) with an AUC of 0.837 versus the NLP model AUC of 0.770 ($p < 0.001$).

Conclusion: A CNN Image Model trained on physiologic lung function data (PFTs) can be applied to chest radiographs for quantitative prediction of obstructive lung disease with good accuracy.

Keywords: machine learning, chronic obstructive pulmonary disease, quantitative image analysis, natural language processing

Introduction

Deep learning techniques are rapidly being applied to medical image interpretation.^{1–3} Multiple studies show convolutional neural network (CNN) models developed to detect specific image features on chest radiographs.^{4–9} Subsequent evaluation of most models asks: “did the CNN model trained on radiologist-labels perform as well or better than the interpreting radiologist?” These approaches to supervised learning require costly and time-consuming “labeling” of disease by radiologists.

Correspondence: Joyce D Schroeder
Department of Radiology and Imaging Sciences, School of Medicine, University of Utah, 30 North 1900 East, Rm #1A71, Salt Lake City, UT 84132, USA
Tel +1 801 581 7553
Fax +1 801 581 2414
Email joyce.schroeder@hsc.utah.edu

We pose the question:

can a CNN model based on physiologic measures of pulmonary disease be used to improve the identification of obstructive lung disease on chest radiograph images compared to the radiologist?

Chest radiographs are, in essence, a “missed screening opportunity” if COPD is present but not described by the radiologist.

COPD is the third leading cause of death worldwide but is often underdiagnosed.^{10–12} Airway inflammation, air trapping and emphysema may be secondary to smoking or environmental exposures and people with COPD are at increased risk of respiratory infections and cancer.¹³ Studies report a twofold to fourfold increase in lung cancer risk in patients with COPD compared to those without airflow obstruction.¹⁴ Lung cancer is the highest mortality cancer in the US and is often discovered at distant stage.¹⁵ The National Lung Screening Trial (NLST) showed a 20% reduction in lung cancer mortality for subjects imaged with CT compared to chest radiograph.¹⁶ However, although lung cancer screening with low-dose computed tomography (LDCT) is now recommended, few patients actually receive CT screening exams: for 2010–2015 fewer than 4% and in 2016 fewer than 2% of those eligible.^{17–19} COPD is typically diagnosed based on PFTs. However, these studies are performed in a minority of individuals at risk. Chest radiographs are the most common imaging study performed worldwide. Identification of individuals with COPD on chest radiographs alone would be a useful adjunct, and, offers an opportunity to target individuals for LDCT screening and/or smoking cessation programs.

Our hypothesis is that a deep learning algorithm trained using chest radiographs with annotation from PFTs (Image Model) will show greater accuracy for the prediction of COPD than text evaluation of the associated radiologist clinical reports (NLP Model, via both bidirectional recurrent neural networks and recent state-of-the-art transformer architecture models).^{20–22} The purpose is to develop a CNN Image model that can be used to augment radiology clinical reports with a quantitative prediction of obstructive lung disease, an important pulmonary disease associated with significant morbidity, mortality and increased risk of lung cancer.

Materials and Methods

Data Acquisition

This study is approved by the University of Utah Institutional Review Board, including a waiver of consent (the research

and privacy risk of the research are no more than minimal), approval for the study plan for patient data confidentiality and compliance with the Declaration of Helsinki. This single-institution retrospective study (Figure 1) uses 6749 two-view chest radiographs, same-day associated radiologist text reports, and near-concurrent PFT exams for 4436 unique subjects. Due to insufficient numbers of subjects with post-bronchodilator PFTs, pre-bronchodilator PFTs are used to enrich the number of cases for training. Inclusion criteria are: pre-bronchodilator PFT exams from 2012 to 2017 with an electronic medical record (EMR) search showing a two-view chest radiograph within 180 days. Subjects with asthma or cystic fibrosis ($n=200$, $<5\%$) are included.²³ Lung transplant subjects are excluded.

For 70% of the study dataset, the PFT is within 15 days of the chest radiograph; other time differences are as follows: 1, 10, 20, 30, 60 and 90 days (51%, 66%, 72%, 79%, 87%, 92%, respectively). Table 1 shows the demographics of the 4436 unique study subjects, the first PFT occurring within the study timeline, and COPD diagnosis code in the EMR if present.

PFTs

All PFTs in the study are pre-bronchodilator values, as used in multiple COPD studies.^{24–26} FEV1 is forced expiratory volume in 1 second. All ‘FEV1’ values reported in this paper are “percent-predicted” (%predFEV1) as provided by the institution’s PFT lab using the National Health and Nutrition Examination Survey (NHANESIII). FVC is forced vital capacity. COPD is defined as FEV1/FVC <0.7 and Global Initiative for Chronic Obstructive Lung Disease (GOLD) stages indicate the severity of disease based on the %predFEV1, ranging from GOLD stage I—mild to GOLD stage IV—very severe.²⁷

Images

Chest radiograph exams in the initial dataset are filtered: 1) both posterior-anterior (PA) and lateral images must be present, 2) exams with greater than two images are excluded, and 3) only the pair of chest radiograph and PFT exams with the smallest date difference is used (maximum date 180 days).

Text

The associated complete radiologist text report, including indication, findings and impression, is acquired for the chest radiograph exams.

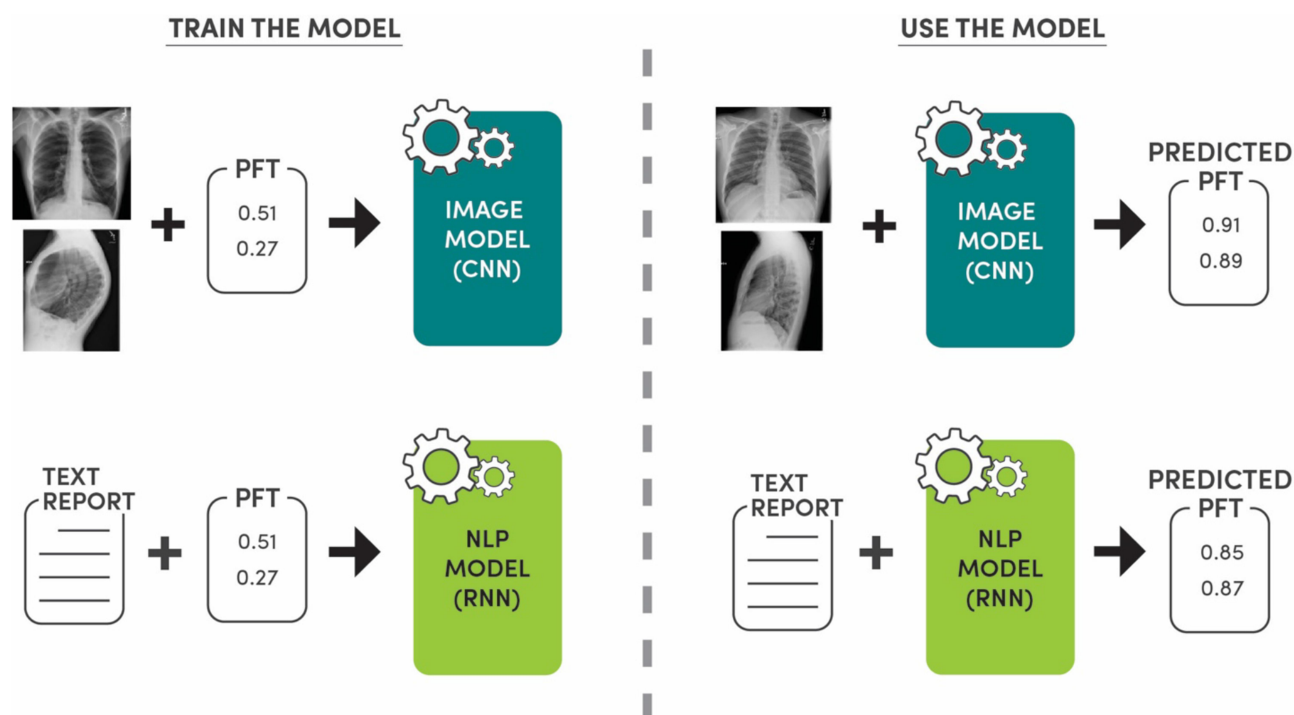


Figure 1 Study overview. The Image Model (CNN = convolutional neural network) is trained using frontal and lateral chest radiograph images and pulmonary function test (PFT) data: FEV1/FVC and FEV1. For 70% of the dataset, the PFT is within 15 days of the chest radiograph, overall within 180 days. The Natural Language Processing (NLP) Model is trained using the associated radiologist text report for the chest radiograph and the PFT data. Two NLP models are used: recurrent neural network (RNN) and state-of-the-art transformer architecture. The Image Model and NLP Model are used in the testing phase to predict PFT values, and therefore the presence or absence of obstructive lung disease.

Dataset

Before filtering is applied, 10% of the subjects are selected for the validation set and 20% for the test set. There are 4436 unique subjects. After filtering, this results in 10% for validation and 19% for testing. The study uses a total of 6749 PFT – Image/Text pairs: 4773 pairs for training, 752 pairs for validation, and 1224 pairs for testing.

Data Preprocessing

Images are cropped using the largest centralized square fitting within the image, resized to 256x256 pixels, and normalized using the mean and standard deviation of the ImageNet dataset.²⁸ The dataset is augmented by horizontal flipping (PA images) and extracting random 224x224 crops. Figure 2 shows an example of original and preprocessed images. The text reports are converted into a sequence of tokens using the spaCy tokenizer (<http://spacy.io/>).

Model Implementation

Image Model

The Image model (Figure 3) uses PA and lateral chest radiographs as inputs to two independent CNNs based on the Resnet-18 model, with weights from a model pretrained on

ImageNet for initialization with the final fully connected layer removed.²⁹ The output layers of both CNNs are concatenated. The resulting vector is used as input to a block of fully connected layers with two hidden layers and softplus output non-linearity. The hidden layers use ReLU activation and dropout (with $p=0.25$).³⁰ The outputs of the model are two positive real values, FEV1/FVC and %predFEV1. The overall model is trained end-to-end with an L1 loss. The batch size is 20, the initial learning rate is 0.0001, and the model is trained for 50 epochs using the Adam optimizer.³¹ The learning rate was reduced by a factor of 10 every time the loss plateaued for 5 epochs.

NLP Model

The NLP pipeline regresses raw text to the same two positive real values, FEV1/FVC and FEV1. We experiment with two strong NLP models: BiLSTM, which represents a standard design of recurrent neural networks, and RoBERTa, which represents recent state-of-the-art transformer architecture.^{20–22}

With the BiLSTM model, we use the Common Crawl version of GloVe embeddings with 100 dimensions, combined with character-level embeddings convoluted by

Table I Demographics, Spirometry and EMR Diagnosis Code for N=4436 Unique Subjects (for Subjects with More Than One PFT Exam, Their First PFT Exam is Reported in This Table)

	Training Set	Validation Set	Test Set	All
Total subjects (%)	3159 (71%)	440 (10%)	837 (19%)	4436 (100%)
No. of subjects				
Normal PFT	2079	289	553	2921 (66%)
GOLD I	254	30	78	362 (8%)
GOLD II	492	78	126	696 (16%)
GOLD III	246	36	53	335 (8%)
GOLD IV	88	7	27	122 (3%)
Age, mean*				
Normal PFT	54.6 (16)	53.5 (17)	54.1 (17)	54.4 (17)
GOLD I	63.9 (15)	66.2 (18)	63.7 (15)	64.0 (15.7)
GOLD II	60.9 (16)	60.0 (15)	60.6 (14)	60.7 (15.7)
GOLD III	60.6 (14)	52.8 (17)	63.1 (15)	60.1 (15.1)
GOLD IV	55.3 (15)	54.9 (22)	56.0 (17)	55.4 (16.1)
Male/Female				
Normal PFT	892/1187	113/176	252/301	1257/1664
GOLD I	146/108	6/24	44/34	196/166
GOLD II	245/247	36/42	65/61	346/350
GOLD III	137/109	14/22	22/31	173/162
GOLD IV	48/40	3/4	14/13	65/57
PFT: FEV1/FVC*				
Normal PFT	0.79 (0.05)	0.79 (0.05)	0.79 (0.06)	0.79 (0.05)
GOLD I	0.65 (0.05)	0.65 (0.05)	0.66 (0.04)	0.66 (0.05)
GOLD II	0.61 (0.07)	0.62 (0.06)	0.61 (0.06)	0.61 (0.07)
GOLD III	0.51 (0.10)	0.53 (0.10)	0.52 (0.11)	0.51 (0.10)
GOLD IV	0.39 (0.12)	0.41 (0.06)	0.40 (0.09)	0.39 (0.12)
PFT: FEV1*				
Normal PFT	0.89 (0.20)	0.91 (0.20)	0.89 (0.21)	0.89 (0.20)
GOLD I	0.91 (0.09)	0.89 (0.09)	0.93 (0.09)	0.91 (0.09)
GOLD II	0.65 (0.09)	0.65 (0.08)	0.65 (0.09)	0.65 (0.09)
GOLD III	0.41 (0.05)	0.42 (0.06)	0.40 (0.06)	0.41 (0.05)
GOLD IV	0.23 (0.04)	0.22 (0.05)	0.23 (0.05)	0.23 (0.04)
COPD diagnosis code present in EMR				
Normal PFT	–	–	–	491 (16.8%)
GOLD I	–	–	–	103 (28.5%)
GOLD II	–	–	–	338 (48.6%)
GOLD III	–	–	–	223 (66.6%)
GOLD IV	–	–	–	86 (70.5%)

Notes: COPD is defined as FEV1/FVC ratio of <0.7 by PFT (spirometry). FEV1 is the amount of air that can be forcibly exhaled from the lungs in the first second of a forced exhalation. FVC is the amount of air that can be forcibly exhaled from the lungs after taking the deepest breath possible. The FEV1/FVC ratio is the percentage of the total amount of air that can be exhaled from the lungs during the first second of forced exhalation. GOLD stages indicate the severity of airflow limitation in COPD. GOLD I (mild): FEV1≥80% predicted, GOLD II (moderate): 50%≤FEV1<80% predicted, GOLD III (severe): 30%≤FEV1<50% predicted, and GOLD IV (very severe): FEV1<30% predicted. *Data in parentheses are ± standard deviation.

Abbreviations: COPD, chronic obstructive pulmonary disease; GOLD, Global Initiative for Chronic Obstructive Lung Disease; PFT, pulmonary function test; EMR, electronic medical record; FEV1, forced expiratory volume in 1 second; FVC, forced vital capacity.

a 2-dimensional filter of size 5.³² The output character encodings of the convolutional network are 100 dimensional. The character encodings and token embeddings (GloVe) are combined by 2-layer highway networks,

resulting in 200-dimensional token-level encodings.³³ Such encodings are then processed by the BiLSTM with the same output dimensionality. The sequence of token encodings is aggregated via self-attention to form

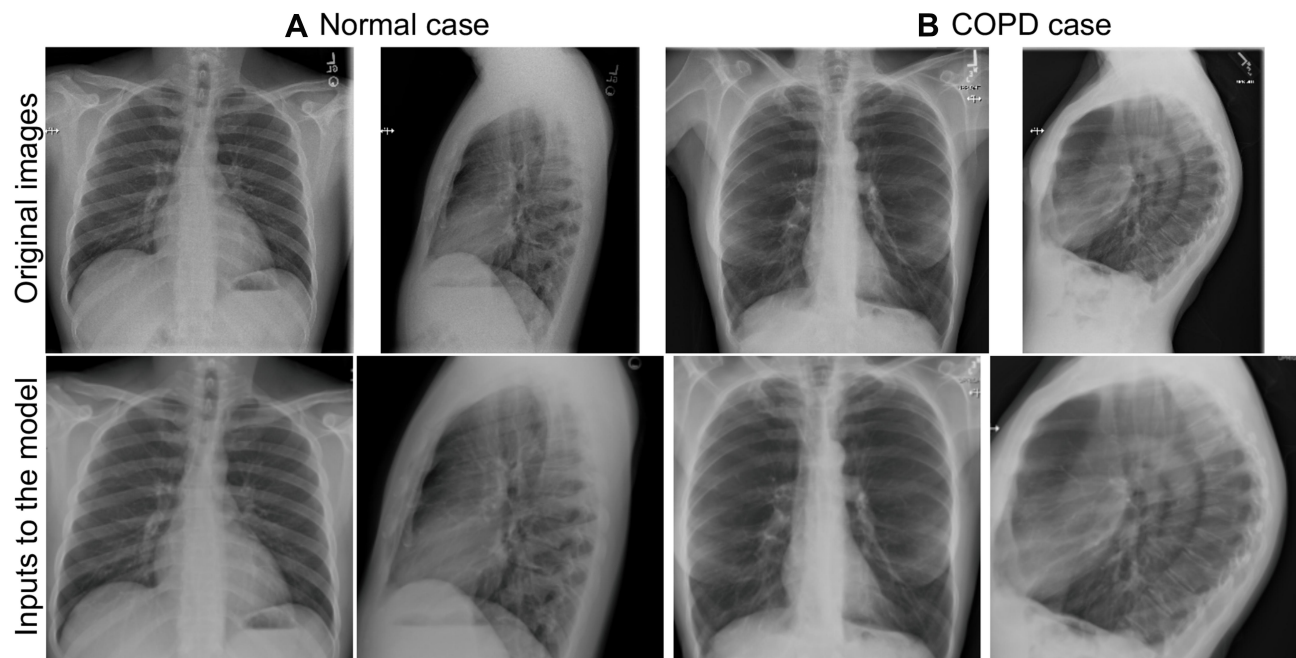


Figure 2 Top row. Example of frontal and lateral chest radiograph images (2048 × 2048 pixels, 12 bits per pixel) for (a) normal case: 36-year-old male, never smoker, pulmonary function test FEV1/FVC = 0.91, FEV1 = 0.89 and (b) COPD case: 62-year-old female, 75 pack-year smoking history, pulmonary function test FEV1/FVC = 0.51, FEV1 = 0.27. The FEV1/FVC ratio is the percentage of the total amount of air that can be exhaled from the lungs during the first second of forced exhalation. In COPD (FEV1/FVC <0.7), air is trapped in the lungs resulting in high lung volumes, flattened hemidiaphragms, increased retrosternal clear space, vascular pruning and lucent lungs as demonstrated in (b) images. Bottom row. Associated pre-processed images used as inputs to the deep learning image model (224 × 224 pixels, 8 bits per pixel) for the example (a) normal case and (b) COPD case. ImageNet normalization is not included for visualization purposes.

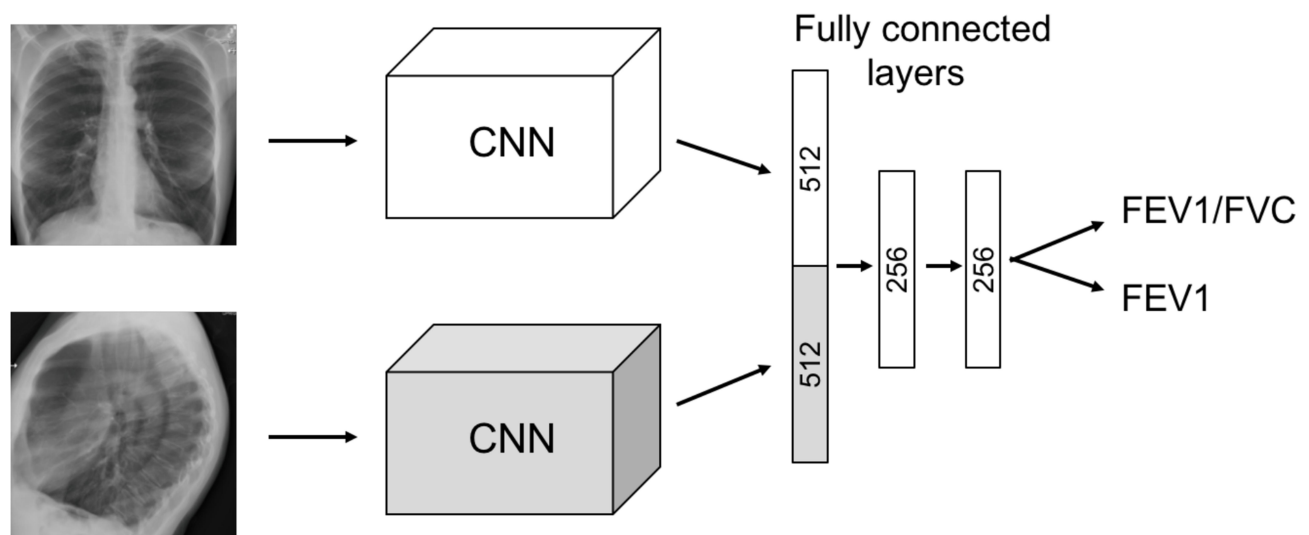


Figure 3 Image model architecture. The frontal and lateral images are inputs to two parallel convolutional neural networks (CNN) trained with annotation data from pulmonary function tests (PFTs). The outputs of the model are the PFT values FEV1/FVC and %predFEV1. The FEV1/FVC ratio is the percentage of the total amount of air that can be exhaled from the lungs during the first second of forced exhalation. FEV1 is the amount of air that can be forcibly exhaled from the lungs in the first second of a forced exhalation, while %predFEV1 is the FEV1 expressed as percent predicted value.

a representation of the entire text, which is fed into a single linear layer with a soft plus activation for the final regression output. For training, the model parameters and character-level embeddings were initialized randomly with uniform distribution (with gain=1).³⁴ We train this

model for 50 epochs with learning rate 0.0001 and dropout rate 0.1 using the Adam optimizer.^{35,36}

With the RoBERTa model, we fine-tuned the pre-trained language model for this task. We used the base version of RoBERTa and take the encoding of the CLS

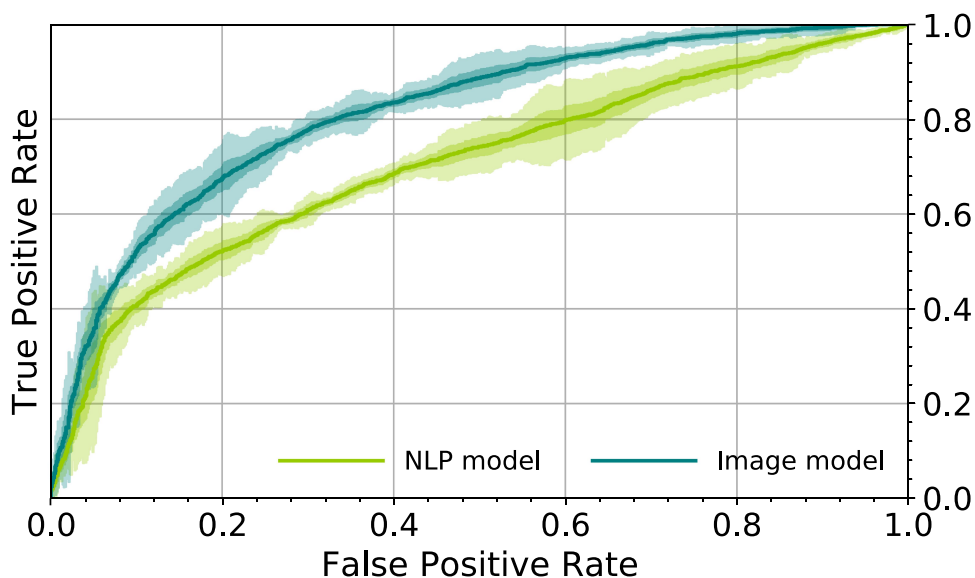


Figure 4 Receiver operator characteristic (ROC) curves for the trained models using a FEV1/FVC threshold of 0.7 for ground-truth. COPD is defined as FEV1/FVC <0.7. The Image model is based on frontal and lateral chest radiographs. The Natural language processing (NLP) model is based on the associated radiologist text reports. The average for five models is shown in the darker color line and one and three standard deviations of the results are shown in the lighter color bands.

token at the final layer as the text representation vector. This representation forms the input to a regression layer that has the same design as in the BiLSTM model. For training, we fine-tuned the model for 20 epochs with learning rate 0.000005, optimized by AdamW with a warm-up percent of 20%.³⁷ The dropout rate for hidden states within the transformer model and before the last linear layer is 0.3.

During training, for both models, we choose the version with the best performance on the development set and report their results on the test set accordingly. We used grid search over the validation set to find the hyperparameters mentioned above.

Statistical Analysis

All models are trained with five different random seeds in order to assess the variability of results with the proposed approach. We compared the Image and NLP models using AUC (area under the receiver operating characteristic curve), accuracy and R^2 , with AUC as the primary metric. For FEV1/FVC, AUC and accuracy are measured by setting a threshold, FEV1/FVC <0.7, as a positive label for COPD diagnosis. For %predFEV1, AUC is measured by setting a threshold, FEV1 <0.5 (GOLD stage severe to very severe), only for cases that are classified as having COPD in the ground-truth. We compared the AUCs from the Image and NLP models using DeLong's method for comparing two correlated ROC curves (pROC package in

R version 3.6.1) with $P < 0.05$ considered a statistically significant difference. Bland–Altman plots are also provided.

Results

Mean age, sex ratios, and initial PFT values are similar between the training, validation and test datasets (Table 1). For the 4436 unique subjects, 66% show normal PFT values (2921) and 34% show obstructive lung disease by PFT values (GOLD stages I–IV total: 1515). The distribution of severity of disease by GOLD stages I–IV (mild to very severe) is 8%, 16%, 8% and 3%, respectively. Male/female ratios are similar for spirometry with normal PFT values and obstructive lung disease, the overall study ratio is 46% male/54% female. The mean age of subjects with normal PFTs (54.4) is lower than the mean age of subjects with disease severity GOLD stage I–III (64.0, 60.7, 60.1) but similar to subjects with GOLD stage IV (55.4).

Table 1 shows that less than half (49.5%) of subjects with PFTs indicating obstructive lung disease (GOLD stages I–IV total: 1515) had a diagnosis code of COPD in the EMR (GOLD stages I–IV total: 750). Diagnosis codes for COPD are present at higher levels for more severe disease: for GOLD stages I–IV the percentage of COPD diagnosis codes is 28.5%, 48.6%, 66.6% and 70.5%, respectively.

All reported results, including the scatter plots, are generated using the test set.

Table 2 Results for Chosen Metrics for All Trained Models

Metric	Image Model	NLP Model
AUC FEV1/FVC	0.814±0.005	0.704±0.010
Accuracy for COPD	0.749±0.008	0.669±0.016
R ² FEV1/FVC	0.415±0.016	0.185±0.013
Specificity FEV1/FVC	0.832±0.025	0.745±0.084
Sensitivity FEV1/FVC	0.630±0.040	0.563±0.082
AUC FEV1	0.837±0.003	0.770±0.007
R ² FEV1	0.512±0.004	0.348±0.013

Notes: Average results ± standard deviations are reported. The Image model is based on frontal and lateral chest radiographs. The NLP model is based on the associated radiologist text reports. FEV1 is the amount of air that can be forcibly exhaled from the lungs in the first second of a forced exhalation. FEV1/FVC is the percentage of total amount of air exhaled from the lungs during the first second of forced exhalation. Accuracy is determined for the COPD/Normal binary classification task. COPD is defined as FEV1/FVC ratio of <0.7. This threshold is used to define positive (COPD) and negative (normal) classes for calculating AUC, sensitivity, specificity and accuracy metrics. All reported results are generated using the test set.

Abbreviations: NLP, natural language processing; AUC, area under receiver operator characteristics curve; COPD, chronic obstructive pulmonary disease; FEV1, forced expiratory volume in 1 second; FVC, forced vital capacity.

Performance of the Image Model

Figure 4 shows the receiver operating characteristic (ROC) curve for the trained Image Model using an FEV1/FVC threshold of 0.7 for ground-truth with COPD defined as FEV1/FVC <0.7. The average for five models trained with

different random seeds is shown in the darker color line and one standard deviation of the results is shown in the lighter color band. The Image Model trained on PFT data results in good prediction of COPD from two-view chest radiograph exams (AUC 0.814±0.005) where AUC is area under the ROC curve. Accuracy for COPD is 0.749±0.008 and R² FEV1/FVC is 0.415±0.016 (Table 2).

A confusion matrix for the Image Model in Table 3 shows the results of classification for different severities of disease (GOLD stages I–IV). The diagonal represents the line where all cases would be located if the model is perfect. The Image Model predicts normal PFTs for most actual normal cases (ground-truth from PFTs). There are 596.0±18.0 predicted normal cases with misclassifications mostly of mild to moderate COPD (GOLD stage I: 24.2±6.9 cases and GOLD stage II: 80.4±14.0 cases), few misclassifications of severe disease (GOLD stage III: 15.4±1.5) and no misclassifications of very severe disease (GOLD stage IV: 0±0.0). For mild to moderate COPD, most misclassifications result in the Image Model predicting normal instead of COPD: 55.0±4.3 cases for GOLD stage I and 80.2±11.4 for GOLD stage II. For severe and very severe COPD, most misclassifications by the Image Model still indicate COPD but one GOLD stage lower

Table 3 Test Set Evaluation: Confusion Matrices for the Image Model (Number of Chest Radiograph Cases by Predicted GOLD Stage) and the NLP Model (Number of Text Report Cases by Predicted GOLD Stage) for All PFT Exam/Chest Radiograph Exam Pairs from the Test Set, N=1224

		GOLD Stage Predicted by the Image Model				
		Normal	I	II	III	IV
Ground-truth from PFT	Normal	596±18.0 (83.2%)	24.2±6.9 (3.4%)	80.4±14.0 (11.2%)	15.4±1.5 (2.2%)	0±0 (0.0%)
	I	55.0±4.3 (61.1%)	12.6±1.5 (14.0%)	21.2±1.9 (23.6%)	1.2±1.3 (1.3%)	0±0 (0.0%)
	II	80.2±11.4 (43.1%)	14.6±1.8 (7.8%)	78.8±8.2 (42.4%)	12.4±2.7 (6.7%)	0±0 (0.0%)
	III	48.2±4.5 (33.7%)	2.6±1.1 (1.8%)	48.6±3.1 (34.0%)	39.2±2.9 (27.4%)	4.4±1.5 (3.1%)
	IV	4.4±2.1 (4.9%)	0.4±0.9 (0.4%)	11.4±4.0 (12.8%)	63±7.6 (70.8%)	9.8±3.7 (11.0%)
		GOLD Stage Predicted by the NLP Model				
		Normal	I	II	III	IV
Ground-truth from PFT	Normal	533.4±59.9 (74.5%)	15.8±22.9 (2.2%)	147.6±45.6 (20.6%)	19.2±6.5 (2.7%)	0±0 (0.0%)
	I	64.2±7.9 (71.3%)	3.0±3.7 (3.3%)	22.2±5.1 (24.7%)	0.6±0.5 (0.7%)	0±0 (0.0%)
	II	96.6±17.6 (51.9%)	2.6±2.9 (1.4%)	68.6±17.3 (36.9%)	18.2±5.0 (9.8%)	0±0 (0.0%)
	III	53±14.2 (37.1%)	1.8±1.9 (1.3%)	52.8±11.4 (36.9%)	35.4±7.8 (24.8%)	0±0 (0.0%)
	IV	8.4±2.9 (9.4%)	0±0 (0.0%)	35.6±9.0 (40.0%)	45±10.2 (50.6%)	0±0 (0.0%)

Notes: The Image model is based on frontal and lateral chest radiographs. The NLP model is based on the associated radiologist text reports. Reported total numbers differ from Table 1, because each subject may be associated with more than one PFT exam/chest radiograph report pair. Average results ± standard deviations (percentage of cases for each ground-truth label) are reported. COPD is defined as FEV1/FVC ratio of <0.7. Normal = FEV1/FVC ratio of ≥0.7. GOLD stages indicate the severity of airflow limitation in COPD. GOLD I (mild): FEV1≥80% predicted, GOLD II (moderate): 50%≤FEV1<80% predicted, GOLD III (severe): 30%≤FEV1<50% predicted, and GOLD IV (severe): FEV1<30% predicted.

Abbreviations: NLP, natural language processing; COPD, chronic obstructive pulmonary disease; GOLD, Global Initiative for Chronic Obstructive Lung Disease; PFT, pulmonary function test.

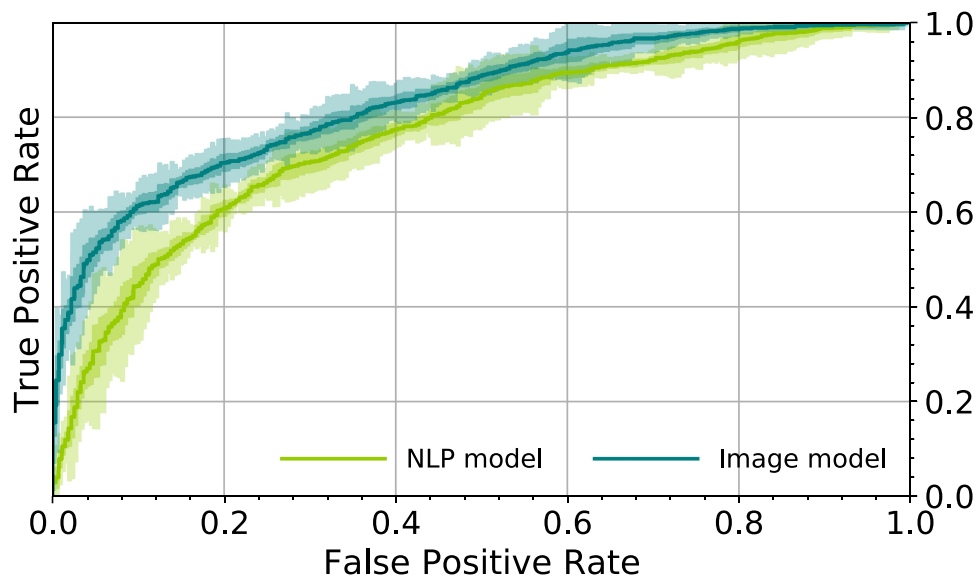


Figure 5 Receiver operator characteristic (ROC) curves for the trained models using a FEV₁ threshold of 0.5 for ground-truth. COPD GOLD stage III or IV disease (severe to very severe airflow limitation) is defined as %predFEV₁ < 50%. The Image model is based on frontal and lateral chest radiographs. The Natural language processing (NLP) model is based on the associated radiologist text reports. The average for five models is shown in the darker color line and one and three standard deviations of the results are shown in the lighter color bands.

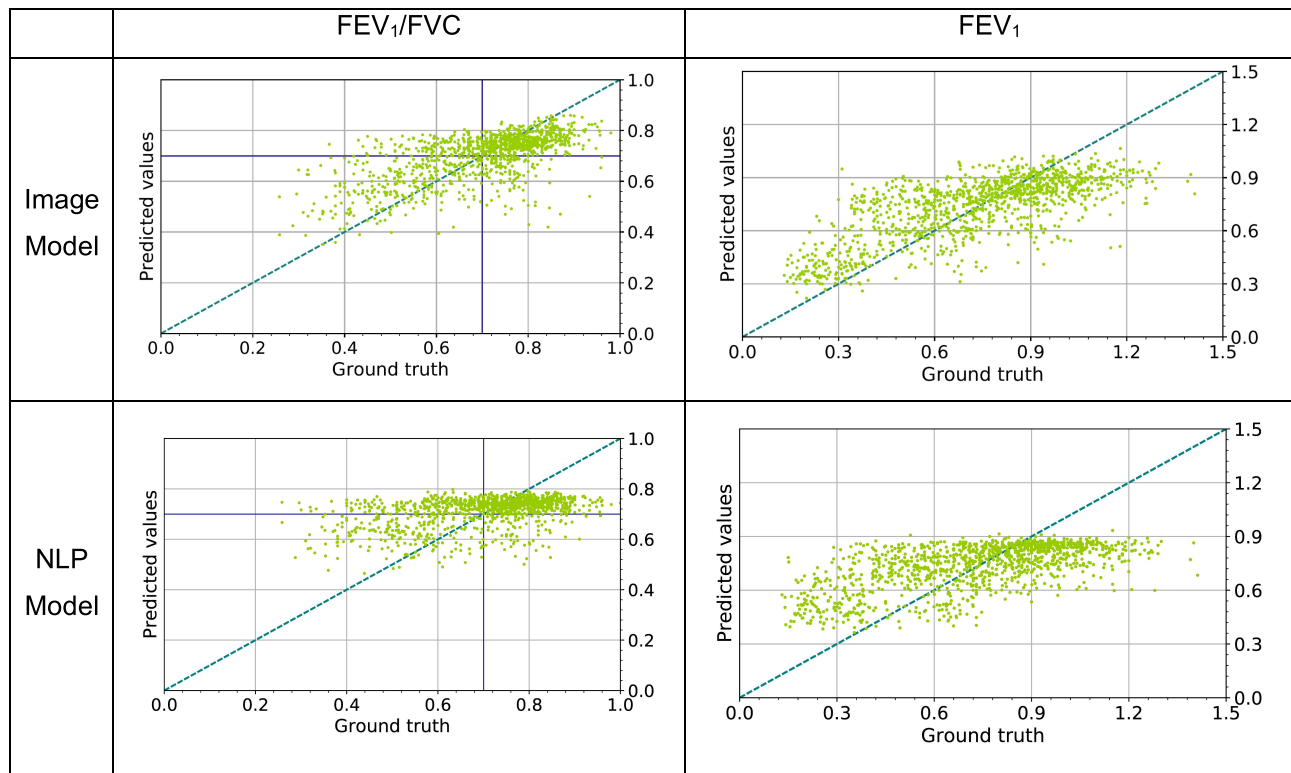


Figure 6 Scatter plots showing the results of regression of the trained models on the test set. The Image model is based on frontal and lateral chest radiographs. The Natural language processing (NLP) model is based on the associated radiologist text reports. The blue dashed line represents the line where all points would be located if the model is perfect. The purple lines represent the threshold for COPD, defined as FEV₁/FVC < 0.7.

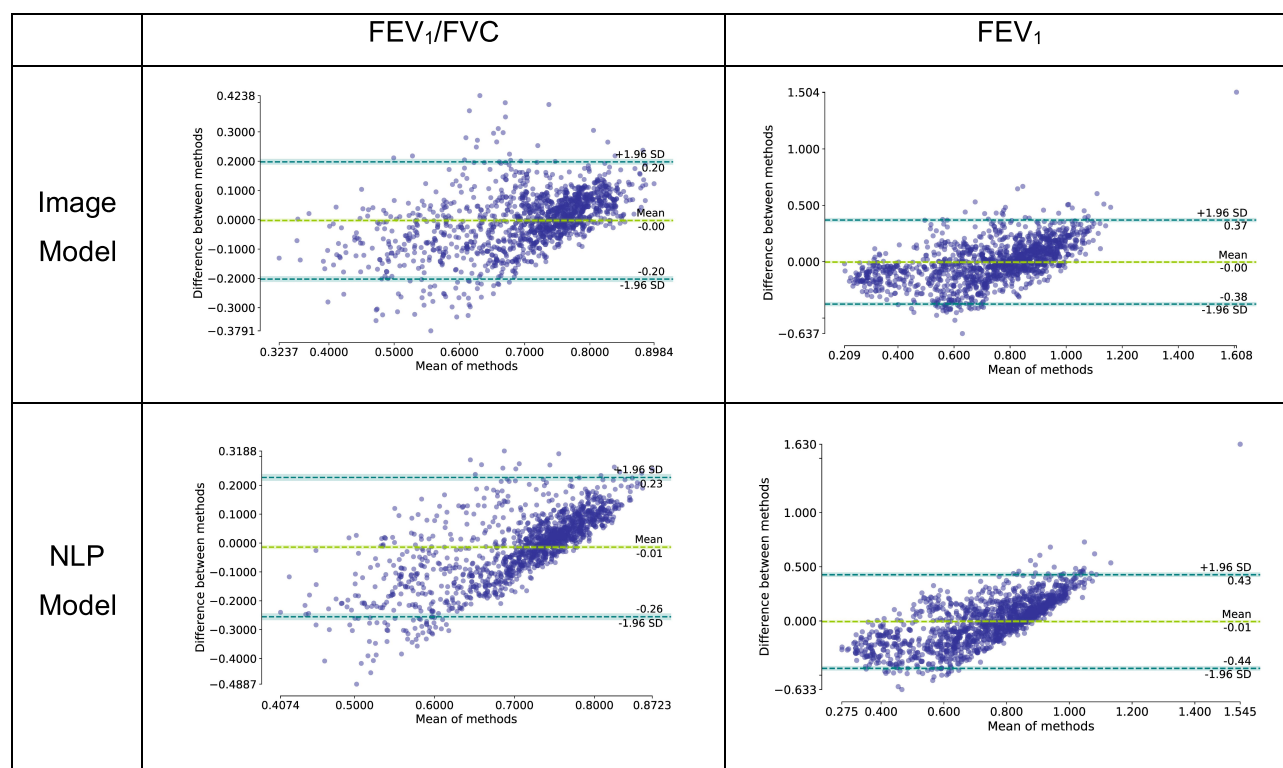


Figure 7 Bland–Altman plots showing the error of the trained models on the test set as a function of the average between ground-truth and model prediction. The blue dashed lines represent 1.96 standard deviations from the average for the error data points, while the green line represents the average error. These graphs are plotted using the library pyCompare (jaketmp/pyCompare v1.5.1; <http://doi.org/10.5281/zenodo.4001461>).

than the ground-truth stage. For actual GOLD stage III, the Image Model predicts 48.6 ± 3.1 cases of GOLD stage II. For actual GOLD stage IV, the Image Model predicts 63.0 ± 7.6 cases of GOLD stage III.

Figure 5 shows the ROC curve for the trained Image Model using a %predFEV1 threshold of 50% for ground-truth, only for cases classified as having COPD in the ground-truth. %predFEV1 <50% is GOLD stage III or IV (severe to very severe disease). This evaluates the Image model in the task of determining the severity of disease, assuming that we know the subject has COPD. The AUC is 0.837 ± 0.003 for determination of severe disease with R^2 FEV1 0.512 ± 0.004 (Table 2).

Figures 6 and 7 show scatter plots and Bland–Altman plots of the results of the Image Model for both output variables: FEV1/FVC and %predFEV1. When evaluating the training dataset only, the model had an R^2 FEV1/FVC of 0.922 ± 0.004 and an R^2 FEV1 of 0.937 ± 0.007 , highlighting a gap between testing scores and training scores. The choice of small CNN depth for the tested model is related to the pronounced overfitting of the model when using deeper architectures and validating on the validation dataset. More training data, in theory, could help in

reducing the gap between training scores and validation/test scores and allow the use of deeper architectures.

Performance of the NLP Model

Figure 4 shows the corresponding ROC curve for the trained NLP Model using an FEV1/FVC threshold of 0.7 for ground-truth with COPD defined as FEV1/FVC <0.7. The NLP Model trained on PFT data results in moderate prediction of COPD (AUC 0.704 ± 0.010). Accuracy for COPD is 0.669 ± 0.016 and R^2 FEV1/FVC is 0.185 ± 0.013 with less predictive metrics compared to the Image Model (Table 2).

The confusion matrix for the NLP Model (Table 3) shows greater numbers of misclassified cases by GOLD stage severity that are at least two GOLD stages different from the ground-truth compared to the Image Model.

The corresponding ROC curve for the NLP Model in determining severe to very severe COPD in subjects with known COPD is shown in Figure 5. The AUC %predFEV1 is 0.770 ± 0.007 and R^2 %predFEV1 is 0.348 ± 0.013 . NLP Model metrics are less predictive for obstructive lung disease compared to the Imaging Model.

Scatter plots and Bland–Altman plots of the results of the NLP Model in Figures 6 and 7 show the predictions of

the NLP model for both output variables: FEV1/FVC and %predFEV1.

One preliminary version of the NLP Model also evaluated common keywords related to COPD in radiologist text reports, by frequency including “emphysema”, “hyperinflation”, “COPD”, ‘flattened diaphragms’, and “vascular pruning”, with frequency order determined by radiologist chest radiograph text report search (Nuance mPower by Montage, 2018.) The keywords did not improve the model and are not a part of the final results.

Comparison of the Image Model and the NLP Model

Differences between Image Model and NLP Model AUCs are statistically significant, $P < 0.001$, for prediction of obstructive lung disease (FEV1/FVC < 0.7) and severe to very severe GOLD stage III–IV disease (%predFEV1 $< 50\%$) using DeLong’s test for two correlated ROC curves. We also tested if the averages of the squared errors of the Image and NLP regression models are different, since regression is used directly instead of classification, with paired Wilcoxon test results $P < 0.001$ for both FEV1/FVC and FEV1.

Figures 6 and 7 show that both models, to different extents, predict values towards the mean when compared with the ground-truth in the extremes of the range of values.

Discussion

The results of this investigation strongly support our hypothesis that a deep learning (DL) algorithm trained using chest radiograph images with annotations from near-concurrent physiologic measures of lung function shows greater accuracy for the prediction of COPD than NLP evaluation of the associated radiologist clinical text reports. Implications of our findings include:

Physiologic measures of pulmonary function can be used to train CNNs for identification of obstructive lung disease on imaging. Labeling datasets with physiologic parameters avoids the time-consuming labeling and interpretation tasks by the radiologist. More importantly, it eliminates the inherent bias and limitations in these radiologist labels. For example, radiologist labels of “emphysema” used in other labeling studies may be ambiguous, describing features of lucent lungs, which may be secondary to either emphysema or air trapping from small airways disease. Physiologic parameters provide a gold

standard, with less bias, and allow the algorithm to evaluate for imaging features that may not be assessed by the radiologist. In the case of COPD, pulmonary function tests, specifically the FEV1/FVC ratio, define the presence and severity of COPD in the appropriate clinical setting per the World Health Organization.²⁷ For those with airflow obstruction, severity is determined by the % predFEV1. Radiographic imaging features of obstructive lung disease, including high lung volumes (hyperinflation), flattened hemi-diaphragms, increased retrosternal clear space, and upper lung predominant lucency and vascular pruning are low spatial resolution features that are not lost in the image downsizing required for inputs to the CNN (Figure 2).

An Image Model CNN for prediction of COPD can add information to augment the radiologist report. The Image Model demonstrates better prediction for COPD compared to the NLP Model from radiologist text reports, suggesting that the DL Image Model can be used to augment the radiologist text reports by generating a prediction of COPD, when present. There are multiple reasons why radiologist reports may not include text indicating COPD. Exams are ordered for other indications (eg, “rule out pneumonia”) and COPD features, particularly if not severe, may not be recognized or assessed. Chest radiographs are a high-volume modality with often narrow indication, eg, “trauma”, and clinical service demands may require short, very directed reports. It is also possible that radiologists may not recognize airflow obstruction in many instances.

Deep learning can be used to consider routine chest radiographs a “screening opportunity” for obstructive lung disease. Our results show that a DL Image Model, while not perfect, improves detection of obstructive lung disease compared to current practice. By generating a numeric metric of disease (predicted FEV1/FVC), the routine chest radiograph can be considered a screening opportunity for COPD. Results can be used to direct patients to medical care of COPD, lung cancer screening (for those meeting age and smoking history criteria) or smoking cessation programs.

Our observations on the performance of PFT annotation for the CNN Image Model compare favorably to other relevant studies using deep learning. Radiologist-labels for “emphysema” are used in these studies to develop networks with reported AUC values of 0.815, 0.829, and 0.926 for the detection of emphysema.⁴ Our findings of significant under-diagnosis of COPD, with less than 50%

of the subjects with COPD by spirometry (PFTs) having a COPD diagnosis code in the EMR in our study population, are similar to other studies.¹⁰

The limitations of this study include the study size, single-institution cohort, and time difference between the chest radiographs/text reports and the PFT exam (up to 180 days). Our study uses pre-bronchodilator PFTs to enrich the number of cases for training which does not distinguish between obstructive lung disease from COPD (emphysema or bronchitis) and that from asthma. Furthermore, our FEV1/FVC <0.7 threshold does not exclude patients with “mixed” lung disease—those with both obstructive and restrictive lung disease, eg, COPD and pulmonary fibrosis. The selection of the maximum 180-day date difference was made to increase the number of cases in the study. Although this time difference introduces the possibility of an acute illness, eg acute exacerbation or pneumonia, that is present on one modality but not the other, we found slightly improved DL Image Model performance with 180-day date difference than with 2-day and 10-day date differences because of the added number of training cases (not shown). Large, diverse multi-institutional cohorts will be required to evaluate the generalizability of the CNN Image Model.

Conclusion

In summary, our study findings show improved prediction of COPD for a CNN Image Model trained with physiologic data (PFTs) compared to NLP Model evaluation of radiologist text reports trained with PFTs. This comparison of models, to our knowledge, is a novel approach for assessing the identification of obstructive lung disease on chest radiographs. Our study conclusions using deep learning to numerically predict airflow obstruction on routine chest radiographs support the goal of better detection of disease. Results suggest that a CNN model trained on physiologic lung function data can be used to augment the clinical radiologist report for improved identification of COPD, an under-diagnosed disease and risk factor for lung cancer.

Acknowledgments

We thank Mike Mitchell (Pulmonary Lab), Associate Professor Angela Presson (Division of Epidemiology), Matt Zabriskie (Radiology Research) and Mingyuan Zhang (Medical Informatics) at the University of Utah for their contributions. The support and resources from the Biomedical Image and Data Analytics Core, the

Scientific Computing and Imaging Institute, and the Center for High Performance Computing at the University of Utah are gratefully acknowledged.

Disclosure

Dr Robert Paine III reports grants from NHLBI, COPD Foundation, and Department of Veterans Affairs; personal fees from Partner Therapeutics, outside the submitted work. The authors report no other conflicts of interest in this work.

References

- Litjens G, Kooi T, Bejnordi BE, et al. A survey on deep learning in medical image analysis. *Med Image Anal.* 2017;42:60–88. doi:10.1016/j.media.2017.07.005
- Havaei M, Davy A, Warde-Farley D, et al. Brain tumor segmentation with deep neural networks. *Med Image Anal.* 2017;35:18–31. doi:10.1016/j.media.2016.05.004
- Ngo TA, Lu Z, Carneiro G. Combining deep learning and level set for the automated segmentation of the left ventricle of the heart from cardiac cine magnetic resonance. *Med Image Anal.* 2017;35:159–171. doi:10.1016/j.media.2016.05.009
- Rajpurkar P, Irvin J, Zhu K, et al. Chexnet: radiologist-level pneumonia detection on chest x-rays with deep learning. *CoRR.* 2017.
- Lakhani P, Sundaram B. Deep learning at chest radiography: automated classification of pulmonary tuberculosis by using convolutional neural networks. *Radiology.* 2017;284(2):574–582. doi:10.1148/radiol.2017162326
- Wang X, Peng Y, Lu L, Lu Z, Bagheri M, Summers RM. ChestX-ray8: hospital-scale chest x-ray database and benchmarks on weakly-supervised classification and localization of common thorax diseases. In: The IEEE Conference on Computer Vision and Pattern Recognition (CVPR), Honolulu, HI; 2017.
- Yao L, Poblenz E, Dagunts D, et al. Learning to diagnose from scratch by exploiting dependencies among labels. *CoRR.* 2017.
- Li Z, Wang C, Han M, et al. Thoracic disease identification and localization with limited supervision. In: The IEEE Conference on Computer Vision and Pattern Recognition (CVPR), Salt Lake City, UT; 2018.
- Seah JCY, Tang JSN, Kitchen A, et al. Chest radiographs in congestive heart failure: visualizing neural network learning. *Radiology.* 2019;290(2):514–522. doi:10.1148/radiol.2018180887
- Martinez CH, Mannino DM, Jaimes FA, et al. Undiagnosed obstructive lung disease in the United States. *AnnalsATS.* 2015;12(12):1788–1795. doi:10.1513/AnnalsATS.201506-388OC
- Martinez FJ, O'Connor GT. Screening, case-finding, and outcomes for adults with unrecognized COPD. *JAMA.* 2016;315(13):1333–1334. doi:10.1001/jama.2016.3274
- Quaderi SA, Hurst JR. The unmet global burden of COPD. *Glob Health Epidemiol Genom.* 2018;3(ed4). doi:10.1017/ghg.2018.1
- Chatila WM, Thomashow BM, Minai OA, et al. Comorbidities in chronic obstructive pulmonary disease. *Proc Am Thorac Soc.* 2008;5(4):549–555. doi:10.1513/pats.200709-148ET
- Gonzalez J, Marin M, Sanchez-Salcedo P, Zulueta JJ. Lung cancer screening in patients with chronic obstructive pulmonary disease. *Ann Transl Med.* 2016;4(8):160. doi:10.21037/atm.2016.03.57
- Siegel RL, Miller KD, Jemal A. Cancer statistics, 2018. *CA Cancer J Clin.* 2018;68(1):7–30. doi:10.3322/caac.21442
- The National Lung Cancer Screening Trial Research Team. Reduced lung-cancer mortality with low-dose computed tomographic screening. *N Engl J Med.* 2011;365(5):395–409. doi:10.1056/NEJMoa1102873

17. Moyer VA, LeFevre ML, Siu AL, et al. Screening for lung cancer: U.S. preventative services task force recommendation statement. *Ann Intern Med.* 2014;160(5):330–338. doi:10.7326/M13-2771
18. Jemal A, Fedewa SA. Lung cancer screening with low-dose computed tomography in the United States—2010 to 2015. *JAMA Oncol.* 2017;3(9):1278–1281. doi:10.1001/jamaoncol.2016.6416
19. Pham D, Bhandari S, Oechsli M, et al. Lung cancer screening rates: data from the lung cancer screening registry. *J Clin Oncol.* 2018;36(15_suppl):6504. doi:10.1200/JCO.2018.36.15_suppl.6504
20. Hochreiter S, Schmidhuber J. Long short-term memory. *Neural Comput.* 1997;9(8):1735–1780. doi:10.1162/neco.1997.9.8.1735
21. Schuster M, Paliwal KK. Bidirectional recurrent neural networks. *IEEE Trans Signal Process.* 1997;45(11):2673–2681. doi:10.1109/78.650093
22. Liu Y, Ott M, Goyal N, et al. RoBERTa: a Robustly Optimized BERT Pretraining Approach. *arXiv.* 2019.
23. Regan EA, Hokanson JE, Murphy JR, et al. Genetic epidemiology of COPD (COPDGene) study design. *COPD.* 2011;7(1):32–43. doi:10.3109/15412550903499522
24. Tseng H, Henry TS, Veeraraghavan S, et al. Pulmonary function tests for the radiologist. *RadioGraphics.* 2017;37(4):1037–1058. doi:10.1148/rg.2017160174
25. Tashkin DP, Wang H, Halpin D, et al. Comparison of the variability of the annual rates of change in FEV1 determined from serial measurements of the pre- versus post-bronchodilator FEV1 over 5 years in mild to moderate COPD: results of the lung health study. *Respir Res.* 2012;13(1):70. doi:10.1186/1465-9921-13-70
26. Mannino DM, Diaz-Guzman E, Buist S. Pre- and post-bronchodilator lung function as predictors of mortality in the lung health study. *Respir Res.* 2011;12(1):136. doi:10.1186/1465-9921-12-136
27. Rabe KF, Hurd S, Anzueto A, et al. Global initiative for chronic obstructive lung disease. Global strategy for the diagnosis, management, and prevention of chronic obstructive pulmonary disease: GOLD executive summary. *Am J Resp Crit Care Med.* 2007;176(6):532–555. doi:10.1164/rccm.200703-456SO
28. Russakovsky O, Deng J, Su H, et al. ImageNet large scale visual recognition challenge. *Int J Comput Vis.* 2015;115(3):211–252. doi:10.1007/s11263-015-0816-y
29. He K, Zhang X, Ren S, Sun J. Deep residual learning for image recognition. In: IEEE CVPR, Las Vegas, NV; 2016: 770–778.
30. Hinton GE, Srivastava N, Krizhevsky A, Sutskever I, Salakhutdinov RR. Improving neural networks by preventing co-adaptation of feature detectors. *arXiv.* 2012.
31. Kingma DP, Ba J. Adam: a method for stochastic optimization. Arxiv:1412.6980. 3rd International Conference for Learning Representations, San Diego, CA; 2015.
32. Pennington J, Socher R, Manning C. Glove: global vectors for word representation. In: Proceedings of the 2014 conference on empirical methods in natural language processing (EMNLP), Dohar, Qatar; 2014: 1532–1543).
33. Srivastava RK, Greff K, Schmidhuber J. Highway networks. *arXiv.* 2015.
34. Glorot X, Bengio Y. Understanding the difficulty of training deep feedforward neural networks. Proceedings of the Thirteenth International Conference on Artificial Intelligence and Statistics, JMLR Workshop and Conference Proceedings, Sardinia, Italy; 9:249–256, 2010.
35. Srivastava N, Hinton G, Krizhevshk A, et al. Dropout: a simple way to prevent neural networks from overfitting. *J Mach Learn Res.* 2014;15:1929–1958.
36. Kingma DP, Ba JL. Adam: a method for stochastic optimization. International Conference on Learning Representations (ICLR) 2015. *arXiv.* 2017.
37. Loshchilov I, Hutter F. Decoupled weight decay regularization. International Conference on Learning Representations (ICLR) 2019. *arXiv.* 2019.

International Journal of Chronic Obstructive Pulmonary Disease

Dovepress

Publish your work in this journal

The International Journal of COPD is an international, peer-reviewed journal of therapeutics and pharmacology focusing on concise rapid reporting of clinical studies and reviews in COPD. Special focus is given to the pathophysiological processes underlying the disease, intervention programs, patient focused education, and self management

protocols. This journal is indexed on PubMed Central, MedLine and CAS. The manuscript management system is completely online and includes a very quick and fair peer-review system, which is all easy to use. Visit <http://www.dovepress.com/testimonials.php> to read real quotes from published authors.

Submit your manuscript here: <https://www.dovepress.com/international-journal-of-chronic-obstructive-pulmonary-disease-journal>